CONF-860396--5

MASTER

ENTRY STATES IN SUBBARRIER FUSION

M. L. Halbert, J. R. Beene, D. C. Hensley
Oak Ridge National Laboratory,* Oak Ridge, Tennessee 37831

K. Honkanen,[1] T. Semkow, V. Abenante, D. G. Sarantites
Washington University,** St. Louis, Missouri 63130

CONF-860396--5

DE86 008888

The cross section for fusion of heavy ions below the Coulomb barrier can be orders of magnitude larger than the predictions of models that are quite successful above the barrier.[2] Recent studies of γ-ray multiplicity[3-6] have shown that the average ℓ of the partial waves participating in subbarrier fusion is much higher than expected. The discrepancies become larger as the mass asymmetry of the projectile and target decreases.

We have used the Spin Spectrometer in coincidence with identified products from two reactions leading to the same compound nucleus, ^{164}Yb, to study entry-state angular-momentum effects. The reactions were ^{64}Ni + ^{100}Mo and ^{16}O + ^{148}Sm; the conditions of bombardment are listed in Table 1. The O + Sm energies were chosen to match two of the Ni + Mo compound-nucleus excitation energies. Exit channels were identified by known γ-ray lines from the residual nuclei observed in six Compton-suppressed Ge detectors which replaced a like number of pentagonal NaI units of the Spin Spectrometer. Recording of events was triggered by detection of a "clean" Ge pulse (i.e., no γ ray detected in its surrounding Compton shield).

The cross sections listed in Table 2 are based on the observed yields of the $2^+ \rightarrow 0^+$ transition in ^{162}Yb (2n channel), ^{160}Yb (4n), and ^{158}Er (α2n), and the $17/2^+ \rightarrow 13/2^+$ plus the $9/2^- \rightarrow 5/2^-$ transitions in ^{161}Yb (3n). Corrections were made for internal conversion and angular distribution effects. No significant yield of ^{163}Yb (1n channel) was observed at any energy except 215 MeV, where it was < 1% of the ^{162}Yb 2+ yield. Small amounts of ^{161}Tm (p2n), ^{157}Er (α3n), or other channels might have been present at the level of a few percent each of the total cross section. Fission is unlikely to contribute at these bombarding energies. Thus the fusion cross section shown in Table 2 was obtained by increasing the sum of the four measured cross sections by 5-10%, an estimate confirmed by the statistical-model calculations described below. The points in Fig. 1 show σ_{fus} for both reactions as a function of energy. The full lines represent calculations[7] which incorporate effects of coupling to excited states in both projectile and target;[8] all inelastic couplings with the ground states were included

with the appropriate β_λ taken from experiment. The good agreement of the predicted and measured σ_{fus} as a function of energy is very encouraging.

Near the barrier the predicted ℓ distributions extend to much higher ℓ values when couplings to inelastic channels are included. Examples are shown in Fig. 2 (dashed lines). When such distributions are used as input to the statistical model, the predicted relative cross sections of the various exit channels (dashed lines in Fig. 3) are in reasonable agreement with experiment at the higher energies but not for the lower energies. The experimental absence of the 1n channel is well reproduced: in no case did the calculation predict a 1n cross section as large as 1% of σ_{fus}.

These calculations were carried out with the program PACE2S[9] using the following assumptions for the residual nuclei: (1) a = A/8.5, (2) giant-resonance E1 shape with strength = 100% of classical sum rule, (3) collective E2 strength = 100 W.u., (4) default values of other γ-ray strengths, and (5) yrast lines that provide a realistic representation of the known yrast lines of nuclei near A = 164. The calculations are rather insensitive to reasonable variations in (1) - (4), but can show large discrepancies with experiment if unrealistic yrast lines are adopted.

We now turn to the information obtained from the Spin Spectrometer in coincidence with characteristic lines of ^{162}Yb ($2^+ \rightarrow 0^+$), ^{161}Yb ($17/2^+ \rightarrow 13/2^+$), ^{160}Yb ($2^+ \rightarrow 0^+$), and ^{158}Er ($2^+ \rightarrow 0^+$). The raw data were processed as follows:[10] (1) The NaI pulse heights were corrected for energy response and pulses due to neutrons were excluded. (2) (H,k) arrays in coincidence with each identified Ge peak (and neighboring background) were generated [H = sum of corrected NaI pulse heights, k = number of responding detectors]. (3) (E,M) arrays were obtained by iterative unfolding of the net (H,k) arrays using the measured response function of each detector in the Spectrometer [E = entry-state excitation energy, M = entry-state γ-ray multiplicity]. (4) Corrections to the (E,M) arrays were applied for the gating transition in the Ge, internal conversion, and angular-distribution effects. In addition, distributions for ^{161}Yb were shifted by 3¼ units in M to account for the angular momentum tied up in the $13/2^+$ band head. It should be pointed out that the high background for low-k events causes loss of information for $k \lesssim 4$. Examples of the E, M entry-state distributions are shown in Fig. 4 in comparison with statistical-model calculations.

The calculations give a good account of the Ni + Mo data down to E_{lab} = 220 MeV. Below this energy the most probable M is underestimated (compare Fig. 4e with 4a), and as already noted the predicted 2n yields are too small at low energies (Fig. 3, dashed lines). The source of these discrepancies may be: (a) the input to the model describing the compound system and its decay products (level densities, yrast lines, gamma decay strengths), (b) the entrance-channel partial-wave distribution (σ_ℓ), and/or (c) a fundamental failure of the statistical calculations to account properly for physical effects that might influence the decay (e.g., a long-lived superdeformed state of the composite system which is preferentially populated in a near-symmetric entrance channel[6]).

Fortunately, the first two possibilities can be investigated in a direct and independent fashion. Concerning point (a), we have found that although extreme variation in the level-density parameters or unrealistic choices of the yrast lines can increase the 2n fraction at low energies, it is not possible in this way to obtain agreement with the experimental M distributions. Our study of point (b) was facilitated by the fact that for these systems, the sum of the M distributions is simply related to the entrance-channel spin distribution and can thus be used to construct an "experimental" σ_ℓ distribution. This was done with the usual expression

$$\ell = 2(M-\langle M_S\rangle) + \langle\Delta I_S\rangle\langle M_S\rangle + \langle I_n\rangle\langle x\rangle + I_0,$$

where the first three terms represent, respectively, the angular momentum carried away by the emission of collective γ rays, statistical γ rays, and neutrons, and I_0 is the spin of the band head. The average multiplicity of the statistical γ rays $\langle M_S\rangle$ and the neutrons $\langle x\rangle$, and the average angular momentum carried away per statistical γ ray $\langle\Delta I_S\rangle$ or neutron $\langle\Delta I_n\rangle$, were taken from the statistical-model calculations. The weak α2n channel was ignored. Examples of the resulting σ_ℓ distributions are shown by the full lines in Fig. 2. At 235 MeV, the general features of the σ_ℓ deduced from experiment agree well with those from the channel-coupling model,[7] a big improvement over models without coupling. However, at low energies the channel-coupling model badly underestimates the contribution of the higher partial waves (Fig. 2a) even though it predicts the energy dependence of the total cross section ($\sum_\ell \sigma_\ell$) very well (Fig. 1). Inclusion of transfer channels[8] does not change the σ_ℓ distribution.

These experimentally-deduced σ_ℓ distributions were taken as input to PACE2S to search for effects of type (c); assumptions (1)-(5) were not changed. To compensate for the experimental losses at low k, the full curves of Fig. 2 were filled out on the low side as shown by the dash-dot lines. The resulting exit-channel fractions, shown by the full curves in Fig. 3, reproduce the measurements remarkably well. Furthermore, the E, M arrays are in good agreement with experiment (compare Fig. 4a and 4c). Thus the decay of the composite system produced in the Ni + Mo reaction appears to proceed precisely according to statistical expectations.

The decay of ^{164}Yb formed by the O + Sm reaction is also well reproduced by the same assumptions (1)-(5); it does not matter whether the σ_ℓ are taken from the channel-coupling model or from the experimental M distributions. Figure 5 compares the k distributions for the two reactions at matched excitation energies. It can be shown that the suppression of the high-k yields in the O + Sm reaction is due entirely to its entrance-channel spin distribution. The compound-nucleus decay is therefore completely statistical for both reactions. We conclude that effects such as superdeformed states preferentially populated by the more symmetric system play no role in the reactions we have studied.

---

*Operated by Martin Marietta Energy Systems, Inc. under contract DE-AC05-840R21400 with the U.S. Department of Energy.
**Work supported by U.S.D.O.E. under contract DE-AS02-76ER04052.
[1] Present address: University of Jyväskylä, Jyväskylä, Finland.
[2] M. Beckerman, Phys. Reports 129, 145 (1985).
[3] S. Gil et al., Phys. Rev. C 31, 1752 (1985).
[4] B. Haas et al., Phys. Rev. Lett. 54, 398 (1985).
[5] P. J. Nolan et al., Phys. Rev. Lett. 54, 2211 (1985).
[6] W. Kühn et al., Phys. Rev. Lett. 51, 1858 (1983); A. Ruckelshaus et al., Legnaro Conference 27-31 May 1985.
[7] C. H. Dasso and S. Landowne, program CCFUS, (unpublished).
[8] R. A. Broglia et al., Phys. Lett. 133B, 34 (1983).
[9] Program PACE2, written by A. Gavron, Phys. Rev. C 21, 230 (1980) and private communication; modification PACE2S by J. R. Beene.
[10] M. Jääskeläinen et al., Nucl. Instrum. Methods 204, 385 (1983).

Table 1. Bombarding conditions. Energies are in MeV. E_{lab} is the bombarding energy halfway through the target. E_{cm} is the mean center-of-mass energy in the target weighted according to the variation of yield with beam energy. E_{CN}^* is the weighted mean excitation energy in the compound nucleus ^{164}Yb.

Projectile	Target	E_{beam}	E_{lab}	E_{cm}	E_{CN}^*
^{64}Ni	^{100}Mo	210.0	207.2	127.8	35.3
		215.0	212.2	130.1	37.7
		220.0	217.2	132.8	40.4
		225.0	222.2	135.5	43.2
		235.1	232.3	141.7	49.4
^{16}O	^{148}Sm	71.2	70.3	63.5	40.4
		81.3	80.4	72.6	49.5

Table 2. Cross sections (in mb) for the four dominant exit channels. Energies are in MeV. Uncertainties are about ±15%. The column labeled σ_{fus} is an estimate of the fusion cross section.

System	E_{beam}	2n	3n	4n	α2n	Sum	σ_{fus}
^{64}Ni + ^{100}Mo	210	0.26	<0.07	-	-	0.26	0.27[a]
	215	1.43	0.78	-	-	2.21	2.34
	220	3.26	4.19	-	-	7.46	8.0
	225	6.3	14.2	0.9	-	21.4	23.1
	235	11.0	39.3	18.1	2.3	70.7	77.8
^{16}O + ^{148}Sm	71	22.2	72.7	1.5	5.5	101.9	110.0
	81	6.4	208.9	166.3	35.7	417.2	458.9

[a]Upper limit = 0.34

Figure Captions

Fig. 1. Fusion cross sections as a function of energy. E_{CN}^{*} is the compound nucleus excitation energy. The center-of-mass bombarding energy is also shown for each reaction. The points are from experiment. The full curves are from the channel-coupling model.[7,8] The dashed curve shows the prediction of the Bass model, a typical model without coupling.

Fig. 2. Calculated cross sections as a function of entrance-channel angular momentum. The dashed curves are predictions of the channel-coupling model.[8,9] The full curves are based on experimental M projections, as described in the text. The dash-dot line compensates for experimental data missing at low k.

Fig. 3. Fractional yields of the four principal exit channels as a function of compound-nucleus excitation energy. (a). Reactions of $^{64}Ni + ^{100}Mo$. (b). Reactions of $^{16}O + ^{148}Sm$. The points are experimental. The dashed and full curves are from a statistical-model calculation using as input the dashed and full (+ dash-dot) curves, respectively, of Fig. 2.

Fig. 4. Contour maps of the entry-state populations in E,M space for $^{64}Ni + ^{100}Mo$ at 215 MeV (left) and 235 MeV (right). The successive contours represent intensities of 0.8, 0.6, 0.4, 0.2, and 0.1 of the maximum (central point) for each exit channel. (a, b). Experimental maps unfolded from the measured H, k arrays. (c, d). Predictions of the statistical model with the experimental curves of Fig. 2 as input for σ_{ℓ}. (e, f). Same as c, d except that the dashed curves of Fig. 2 were taken as input for σ_{ℓ}.

Fig. 5. Projections of the experimental H, k distributions onto the k axis for the two reactions at matched compound-nucleus excitation energies. (a). $^{16}O + ^{148}Sm$ at 71 MeV. (b). $^{16}O + ^{148}Sm$ at 81 MeV. (c). $^{64}Ni + ^{100}Mo$ at 220 MeV. (d). $^{64}Ni + ^{100}Mo$ at 235 MeV. The reactions plotted on the left (right) are for $E_{CN}^{*} = 40.4$ (49.4) MeV.

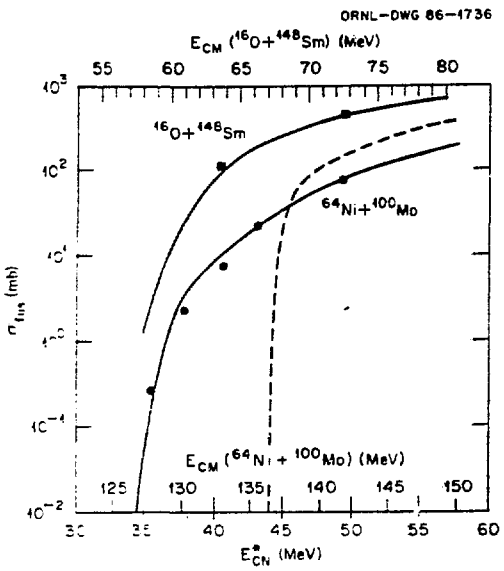

Fig. 1

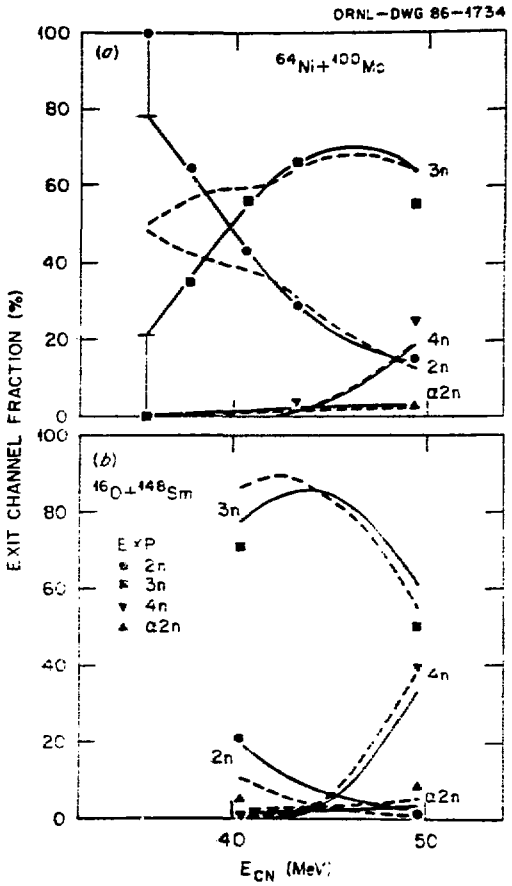

Fig. 3

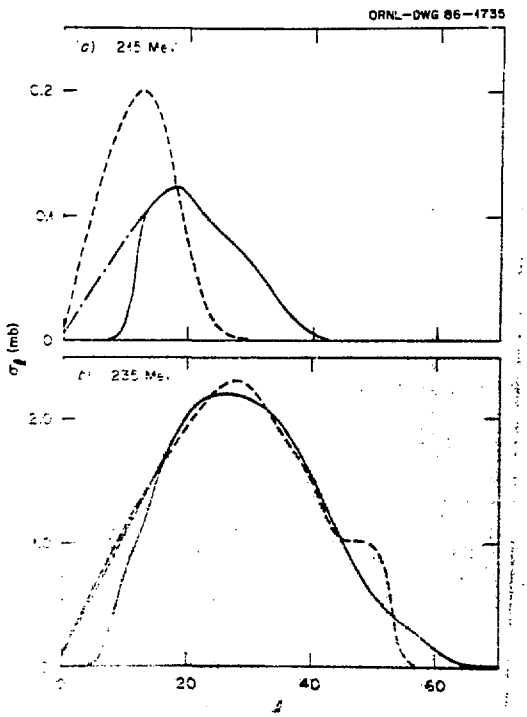

Fig. 2

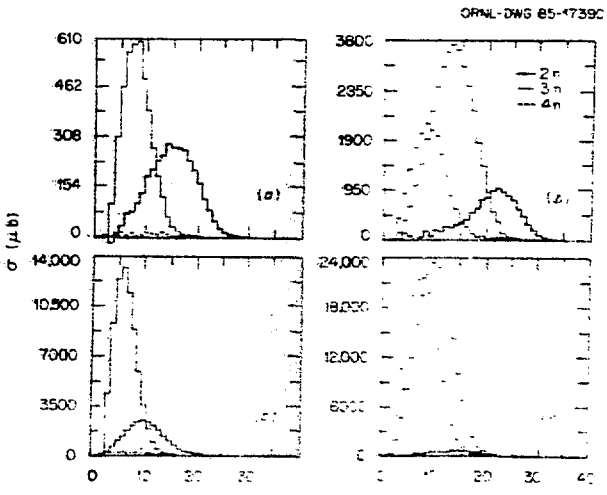

Fig. 5

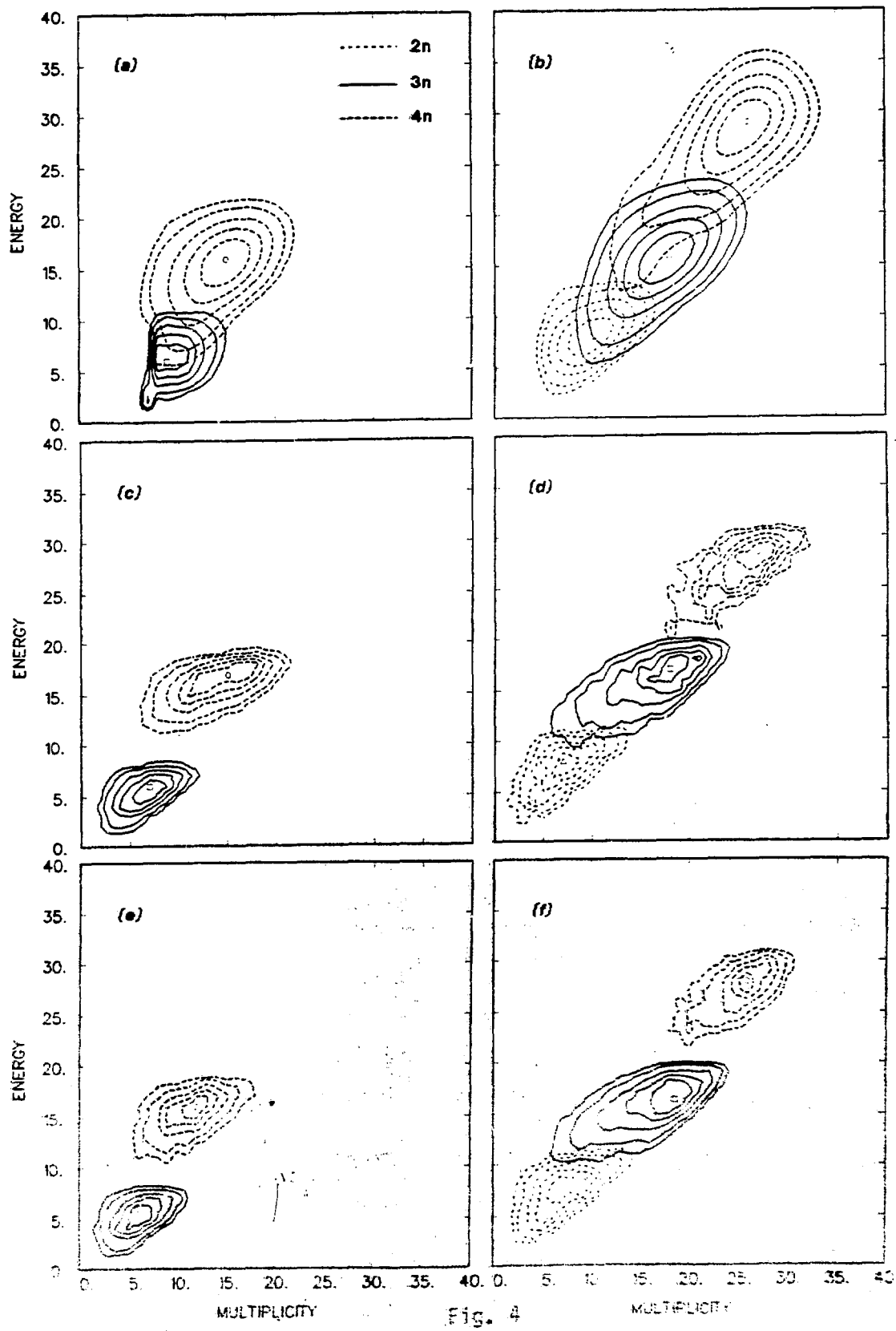

Fig. 4